QCD BOUND STATES AND THEIR RESPONSE TO EXTREMES OF TEMPERATURE AND DENSITY

P. MARIS AND C. D. ROBERTS
Physics Division, Bldg. 203, Argonne National Laboratory
Argonne IL 60439-4843, USA

We describe the application of Dyson-Schwinger equations to the calculation of hadron observables. The studies at zero temperature (T) and quark chemical potential (μ) provide a springboard for the extension to finite-(T,μ). Our exemplars highlight that much of hadronic physics can be understood as simply a manifestation of the nonperturbative, momentum-dependent dressing of the elementary Schwinger functions in QCD.

1 DSE Essentials

The Dyson-Schwinger equations (DSEs) provide a Poincaré invariant, continuum approach to solving quantum field theories. They are an infinite tower of coupled integral equations, with the equation for a particular n-point function involving at least one $m > n$-point function. A tractable problem is only obtained if one truncates the system, and historically this has provided an impediment to the application of DSEs: *a priori* it can be difficult to judge whether a particular truncation scheme will yield qualitatively or quantitatively reliable results for the quantity sought. As integral equations, the analysis of observables is a numerical problem and hence a critical evaluation of truncation schemes often requires access to high-speed computers.[a] With such tools now commonplace, this evaluation can be pursued fruitfully.

The development of efficacious truncation schemes in not a purely numerical task, and neither is it always obviously systematic. For some, this last point diminishes the appeal of the approach. However, with growing community involvement and interest, the qualitatively robust results and intuitive understanding that the DSEs can provide is becoming clear. Indeed, someone familiar with the application of DSEs in the late-70s and early-80s might be surprised with the progress that has been made. It is now clear[1] that truncations which preserve the global symmetries of a theory; for example, chiral symmetry in QCD, are relatively easy to define and implement and, while it is more difficult to preserve local gauge symmetries, much progress has been made with Abelian theories[2] and more is being learnt about non-Abelian ones.

[a] The human and computational resources required are still modest compared with those consumed in contemporary numerical simulations of lattice-QCD.

The simplest truncation scheme for the DSEs is the weak-coupling expansion. It shows that the DSEs *contain* perturbation theory; i.e, for any given theory the weak-coupling expansion generates all the diagrams of perturbation theory. However, the most important feature of the DSEs is the antithesis of this weak-coupling expansion: the DSEs are intrinsically nonperturbative and their solution contains information that is *not* present in perturbation theory. They are ideal for the study of dynamical chiral symmetry breaking (DCSB) and confinement in QCD, and of hadronic bound state structure and properties. In this application they provide a means of elucidating identifiable signatures of the quark-gluon substructure of hadrons.

Their intrinsically nonperturbative nature also makes them well suited to studying QCD at finite-(T,μ), where the characteristics of the phase transition to a quark-gluon plasma are a primary subject. The order of the transition, the critical exponents, and the response of bound states to changes in these intensive variables: all must be elucidated. The latter because there lies the signals that will identify the formation of the plasma and hence guide the current and future experimental searches.

1.1 Gluon Propagator

In Landau gauge the two-point, dressed-gluon Schwinger function, or dressed-gluon propagator, has the form

$$g^2 D_{\mu\nu}(k) = \left(\delta_{\mu\nu} - \frac{k_\mu k_\nu}{k^2}\right) \frac{\mathcal{G}(k^2)}{k^2}\,,\; \mathcal{G}(k^2) := \frac{g^2}{[1+\Pi(k^2)]}\,, \tag{1}$$

where $\Pi(k^2)$ is the vacuum polarisation, which contains all the dynamical information about gluon propagation. Studies of the gluon DSE have been reported by many authors[3] with the conclusion that, if the ghost-loop is unimportant, then the charge-antiscreening 3-gluon vertex dominates and, relative to the free gauge boson propagator, the dressed gluon propagator is significantly enhanced in the vicinity of $k^2 = 0$.[b] The enhancement persists to $k^2 \sim$ 1-2 GeV^2, where a perturbative analysis becomes quantitatively reliable. In the neighbourhood of $k^2 = 0$ the enhancement can be represented[5] as a regularisation

[b]The possibility that $\mathcal{G}(k^2)$ is finite or vanishes at $k^2 = 0$ is canvassed in these proceedings. In the absence of particle-like singularities in the quark-gluon vertex such behaviour is very difficult to reconcile with the observable phenomena of QCD.[4] A particle-like singularity is one of the form $(P^2)^{-\alpha}$, $\alpha \in (0,1]$. In this case one can write a spectral decomposition for the vertex in which the spectral densities are non-negative. This is impossible if $\alpha > 1$. $\alpha = 1$ is the ideal case of an isolated, δ-function singularity in the spectral densities and hence an isolated, free-particle pole. $\alpha \in (0,1)$ corresponds to an accumulation, at the particle pole, of branch points associated with multiparticle production.

of $1/k^4$ as a distribution. A dressed-gluon propagator of this type generates confinement[c] and DCSB *without* fine-tuning.

1.2 Quark Propagator

In a covariant gauge the two-point, dressed-quark Schwinger function, or dressed-quark propagator, can be written in a number of equivalent forms

$$S(p) := \frac{1}{i\gamma\cdot p + \Sigma(p)} \tag{2}$$

$$:= \frac{1}{i\gamma\cdot p\, A(p^2) + B(p^2)} \equiv -i\gamma\cdot p\,\sigma_V(p^2) + \sigma_S(p^2)\,. \tag{3}$$

$\Sigma(p)$ is the dressed-quark self energy, which satisfies

$$\Sigma(p) = (Z_2 - 1)\, i\gamma\cdot p + Z_4\, m_{\rm bm} + Z_1 \int_q^\Lambda g^2 D_{\mu\nu}(p-q)\frac{\lambda^a}{2}\gamma_\mu S(q)\Gamma^a_\nu(q,p)\,, \tag{4}$$

where $\Gamma^a_\nu(q;p)$ is the renormalised dressed-quark-gluon vertex, $m_{\rm bm}$ is the Lagrangian current-quark bare mass and $\int_q^\Lambda := \int^\Lambda d^4q/(2\pi)^4$ represents mnemonically a *translationally-invariant* regularisation of the integral, with Λ the regularisation mass-scale. The quark-gluon-vertex and quark wave function renormalisation constants, $Z_1(\mu^2,\Lambda^2)$ and $Z_2(\mu^2,\Lambda^2)$, depend on the renormalisation point, μ, and the regularisation mass-scale, as does the mass renormalisation constant $Z_m(\mu^2,\Lambda^2) := Z_2(\mu^2,\Lambda^2)^{-1} Z_4(\mu^2,\Lambda^2)$.

The quark mass-function is $M(p^2) := B(p^2)/A(p^2)$ and, as illustrated in Fig. 1,[6] solving the quark DSE using an infrared-enhanced dressed-gluon propagator and a dressed-quark-gluon vertex, $\Gamma_\mu(p,q)$, that does not exhibit particle-like singularities at $(p-q)^2 = 0$, one obtains a quark mass-function that mirrors the infrared enhancement of the dressed-gluon propagator. These results were obtained using the one-loop formula for the running mass, with current-quark masses corresponding to

$$\begin{array}{cccc} m_{u/d}^{1\,\rm GeV} & m_s^{1\,\rm GeV} & m_c^{1\,\rm GeV} & m_b^{1\,\rm GeV} \\ 6.6\,{\rm MeV} & 140\,{\rm MeV} & 1.0\,{\rm GeV} & 3.4\,{\rm GeV}\,. \end{array} \tag{5}$$

The quark DSE was also solved in the chiral limit, which in QCD is obtained by setting the Lagrangian current-quark bare mass to zero.[6] One observes immediately that the mass-function is nonzero even in this case. That

[c]One aspect of confinement is the absence of quark and gluon production thresholds in colour-singlet-to-singlet $\mathcal{S}$-matrix amplitudes. This is ensured if the dressed-quark and -gluon propagators do not have a Lehmann representation.

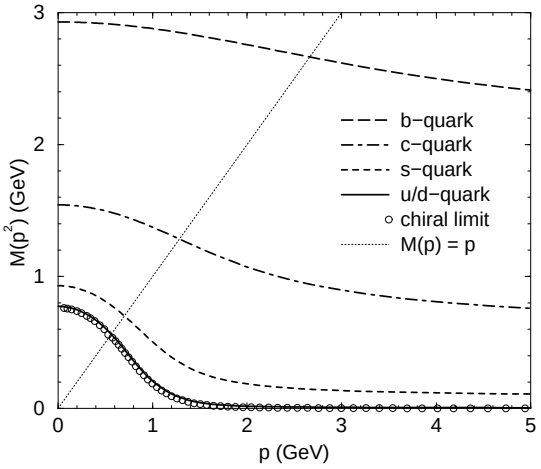

Figure 1: Dressed-quark mass-function obtained in solving the quark DSE.

is DCSB: a momentum-dependent quark mass, generated dynamically, in the absence of any term in the action that breaks chiral symmetry explicitly. This entails a nonzero value for the quark condensate in the chiral limit. That $M(p^2) \neq 0$ in the chiral limit is independent of the details of the infrared-enhanced dressed-gluon propagator.

Figure 1 illustrates that for light quarks (u, d and s) there are two distinct domains: perturbative and nonperturbative. In the perturbative domain the magnitude of $M(p^2)$ is governed by the the current-quark mass. For $p^2 < 1\,\mathrm{GeV}^2$ the mass-function rises sharply. This is the nonperturbative domain where the magnitude of $M(p^2)$ is determined by the DCSB mechanism; i.e., the enhancement in the dressed-gluon propagator. This emphasises that DCSB is more than just a nonzero value of the quark condensate in the chiral limit!

The solution of $p^2 = M^2(p^2)$ defines a Euclidean constituent-quark mass, M^E. For a given quark flavour, the ratio M_f^E/m_f^μ is a single, quantitative measure of the importance of the DCSB mechanism in modifying the quark's propagation characteristics. As illustrated in Eq. (6),

flavour	u/d	s	c	b	t
$\frac{M^E}{m_{\mu\sim 20\,\mathrm{GeV}}}$	150	10	2.3	1.4	$\to 1$

(6)

this ratio provides for a natural classification of quarks as either light or heavy. For light-quarks the ratio is characteristically 10-100 while for heavy-quarks

it is only 1-2. The values of this ratio signal the existence of a characteristic DCSB mass-scale: M_χ. At $p^2 > 0$ the propagation characteristics of a flavour with $m_f^\mu < M_\chi$ are altered significantly by the DCSB mechanism, while for flavours with $m_f^\mu \gg M_\chi$ it is irrelevant, and explicit chiral symmetry breaking dominates. It is apparent from the figure that $M_\chi \sim 0.2\,\mathrm{GeV} \sim \Lambda_{\mathrm{QCD}}$. This forms the basis for simplifications in the study of heavy-meson observables.[7]

1.3 Hadrons: Bound States

The properties of hadrons can be understood in terms of their substructure by studying covariant bound state equations: the Bethe-Salpeter equation (BSE) for mesons and the covariant Fadde'ev equation for baryons. The mesons have been studied most extensively and their internal structure is described by a Bethe-Salpeter amplitude obtained as a solution of

$$[\Gamma_H(k;P)]_{tu} = \int_q^\Lambda [\chi_H(q;P)]_{sr}\, K^{rs}_{tu}(q,k;P)\,, \tag{7}$$

where $\chi_H(q;P) := \mathcal{S}(q_+)\Gamma_H(q;P)\mathcal{S}(q_-)$; $\mathcal{S}(q) = \mathrm{diag}(S_u(q), S_d(q), S_s(q), \ldots)$; $q_+ = q + \eta_P\, P$, $q_- = q - (1-\eta_P)\, P$, with P the total momentum of the bound state and observables independent of η_P; and $r,\ldots,u$ represent colour-, Dirac- and flavour-matrix indices. The amplitude for a pseudoscalar bound state has the form

$$\begin{aligned}\Gamma_H(k;P) = T^H\gamma_5 \Big[& iE_H(k;P) + \gamma\cdot P F_H(k;P) \\ & + \gamma\cdot k\, k\cdot P\, G_H(k;P) + \sigma_{\mu\nu}\, k_\mu P_\nu\, H_H(k;P)\Big]\,,\end{aligned} \tag{8}$$

where T^H is a flavour matrix that determines the mesonic channel under consideration; e.g., $T^{K^+} := (1/2)\left(\lambda^4 + i\lambda^5\right)$, with $\{\lambda^j, j = 1\ldots 8\}$ the Gell-Mann matrices. In Eq. (7), K is the renormalised, fully-amputated, quark-antiquark scattering kernel and important in the successful application of DSEs is that it has a systematic skeleton expansion in terms of the elementary, dressed-particle Schwinger functions; e.g., the dressed-quark and -gluon propagators. This particular expansion,[1] with its analogue for the kernel in the quark DSE, provides a means of constructing a kernel that, order-by-order in the number of vertices, ensures the preservation of vector and axial-vector Ward-Takahashi identities.

In any study of meson properties, one chooses a truncation for K. The BSE is then fully specified and straightforward to solve, yielding the bound

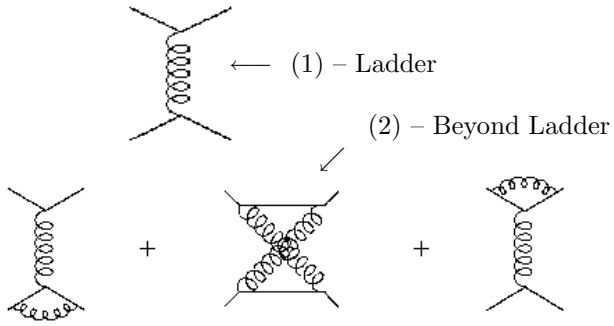

Figure 2: First two orders in a systematic expansion of the quark-antiquark scattering kernel. In this expansion, the propagators are dressed but the vertices are bare.

state mass and amplitude. The "ladder" truncation of K combined with the "rainbow" truncation of the quark DSE [$\Gamma_\mu \to \gamma_\mu$ in Eq. (4)] is the simplest and most often used. The expansion of Fig. 2 provides the explanation[1] for why this Ward-Takahashi identity preserving truncation is accurate for flavour-nonsinglet pseudoscalar and vector mesons: there are cancellations between the higher-order diagrams. It also shows why it provides a poor approximation in the study of scalar mesons, where the higher-order terms do not cancel, and for flavour-singlet mesons, where it omits timelike gluon exchange diagrams.

2 A Mass Formula

The dressed-axial-vector vertex satisfies a DSE whose kernel is K, and because of the systematic expansion described in Sec. 1.3 it follows[6] that the axial-vector Ward-Takahashi identity (AV-WTI):

$$-iP_\mu \Gamma^H_{5\mu}(k;P) = \mathcal{S}^{-1}(k_+)\gamma_5 \frac{T^H}{2} + \gamma_5 \frac{T^H}{2}\mathcal{S}^{-1}(k_-) - M_{(\mu)}\,\Gamma^H_5(k;P) - \Gamma^H_5(k;P)\,M_{(\mu)}\,, \tag{9}$$

[$M_{(\mu)} = \mathrm{diag}(m^\mu_u, m^\mu_d, m^\mu_s, \ldots)$ is the current-quark mass matrix] is satisfied in any thoughtful truncation of the DSEs. That entails many important results.[6]

1) The axial-vector vertex has a pole at $P^2 = -m_H^2$ whose residue is f_H, the leptonic decay constant:

$$f_H P_\mu = Z_2 \int_q^\Lambda \frac{1}{2}\mathrm{tr}\left[\left(T^H\right)^{\mathrm{t}}\,\gamma_5\gamma_\mu \mathcal{S}(q_+)\Gamma_H(q;P)\mathcal{S}(q_-)\right]\,, \tag{10}$$

with the trace over colour, Dirac and flavour indices.

2) In the chiral limit

$$\begin{aligned} &f_H E_H(k;0) = B_0(k^2)\,, && F_R(k;0) + 2\,f_H F_H(k;0) = A_0(k^2)\,,\\ &G_R(k;0) + 2\,f_H G_H(k;0) = 2A_0'(k^2)\,, && H_R(k;0) + 2\,f_H H_H(k;0) = 0\,, \end{aligned} \tag{11}$$

where $A_0(k^2)$ and $B_0(k^2)$ are the solutions of Eq. (4) in the chiral limit, and F_R, G_R and H_R are calculable functions in $\Gamma^H_{5\mu}$. This shows that when chiral symmetry is dynamically broken: 1) the flavour-nonsinglet, pseudoscalar BSE has a massless solution; 2) the Bethe-Salpeter amplitude for the massless bound state has a term proportional to γ_5 alone, with the momentum-dependence of $E_H(k;0)$ completely determined by that of $B_0(k^2)$, in addition to terms proportional to other pseudoscalar Dirac structures that are nonzero in general; and 3) the axial-vector vertex, $\Gamma^H_{5\mu}(k;P)$, is dominated by the pseudoscalar bound state pole for $P^2 \simeq 0$. The converse is also true.

3) The pseudoscalar vertex also has a pole at $P^2 = -m_H^2$ whose residue is

$$ir_H = Z_4 \int_q^\Lambda \frac{1}{2}\mathrm{tr}\left[\left(T^H\right)^{\mathrm{t}} \gamma_5 \mathcal{S}(q_+)\Gamma_H(q;P)\mathcal{S}(q_-)\right] . \tag{12}$$

4) There is an identity between the residues of the pseudoscalar meson pole in the axial-vector and pseudoscalar vertices that is satisfied independent of the magnitude of the current quark mass:

$$f_H\, m_H^2 = r_H\, \mathcal{M}_H\,, \quad \mathcal{M}_H := \mathrm{tr}_{\mathrm{flavour}}\left[M_{(\mu)}\, \left\{T^H, \left(T^H\right)^{\mathrm{t}}\right\}\right] . \tag{13}$$

2.1 Corollaries

Equation (13) is a mass formula for flavour-octet pseudoscalar mesons. For small current-quark masses, using Eqs. (8) and (11), Eq. (12) yields

$$r_H^0 = -\,\frac{1}{f_H^0}\,\langle\bar{q}q\rangle_\mu^0\,, \quad -\langle\bar{q}q\rangle_\mu^0 := Z_4(\mu^2,\Lambda^2)\,N_c \int_q^\Lambda \mathrm{tr}_{\mathrm{Dirac}}\left[S_{\hat{m}=0}(q)\right] , \tag{14}$$

where $\langle\bar{q}q\rangle_\mu^0$ is the chiral limit *vacuum quark condensate*, which is renormalisation-point dependent but independent of the gauge parameter and the regularisation mass-scale:[6] $\langle\bar{q}q\rangle^0_{\mu=1\,\mathrm{GeV}} = -\,(0.241\,\mathrm{GeV})^3$. Now one obtains immediately from Eqs. (13) and (14)

$$f_\pi^2 m_\pi^2 = -\,[m_u^\mu + m_d^\mu]\,\langle\bar{q}q\rangle_\mu^0 + \mathrm{O}\left(\hat{m}_q^2\right) \tag{15}$$

$$f_{K^+}^2 m_{K^+}^2 = -\,[m_u^\mu + m_s^\mu]\,\langle\bar{q}q\rangle_\mu^0 + \mathrm{O}\left(\hat{m}_q^2\right)\,, \tag{16}$$

which exemplify what is commonly known as the Gell-Mann–Oakes–Renner relation. [$\hat{m}_q$ is the renormalisation-point-independent current-quark mass.] In a typical, model calculation[6] Eq. (15) is accurate to 7%, while Eq. (16) receives corrections of 43% from $\mathrm{O}\left(\hat{m}_q^2\right)$ and higher, see Fig. 3.

In the heavy-quark limit, $\eta_P = 1$ in Eq. (7) and the heavy-meson velocity (v_μ) and binding energy (E) are defined via: $P := m_H\, v_\mu$, $v^2 = -1$, $M_H := (\hat{M}_Q + E)$, with M_H the heavy-meson mass and $\hat{M}_Q \approx M_Q^E \approx \hat{m}_Q$; see Sec. 1.2. In this case[7], at leading order in $1/M_H$,

$$S(q+P) = \frac{1}{2}\,\frac{1 - i\gamma\cdot v}{q\cdot v - E}\,, \tag{17}$$

$$\Gamma_H(q;P) = \sqrt{M_H}\,\hat{\Gamma}_H(q;P)\,, \tag{18}$$

where the canonical normalisation condition for $\hat{\Gamma}_H(q;P)$ is independent of M_H. Using Eqs. (17) and (18) in Eq. (10) one obtains

$$f_H \propto 1/\sqrt{M_H} \tag{19}$$

and this along with Eqs. (12) and (13) yields

$$M_H \propto \hat{m}_Q\,. \tag{20}$$

A model study[8] shows Eq. (20) to be valid for $\hat{m}_Q \gtrsim \hat{m}_s$, and this is confirmed by data, Fig. 3. However, both calculations and available data suggest that Eq. (19) is not manifest until $\hat{m}_Q > \hat{m}_c$.

3 Finite T and μ

The study of QCD at finite temperature and baryon number density proceeds via the introduction of the intensive variables: temperature and quark chemical potential. These are additional mass-scales, with which the coupling can *run* and hence, for $T \gg \Lambda_{\rm QCD}$ and/or $\mu \gg \Lambda_{\rm QCD}$, $\alpha_{\rm S}(Q^2 = 0, T, \mu) \sim 0$. It follows that at finite temperature and/or baryon number density there is a phase of QCD in which quarks and gluons are weakly interacting, *irrespective* of the momentum transfer; i.e., a quark-gluon plasma. Such a phase of matter existed approximately one microsecond after the big-bang. In this phase confinement and DCSB are absent and the nature of the strong interaction spectrum is qualitatively different.

Nonperturbative methods are necessary to study the phase transition, which is characterised by qualitative changes in order parameters such as the quark condensate. One widely used approach is the numerical simulation of

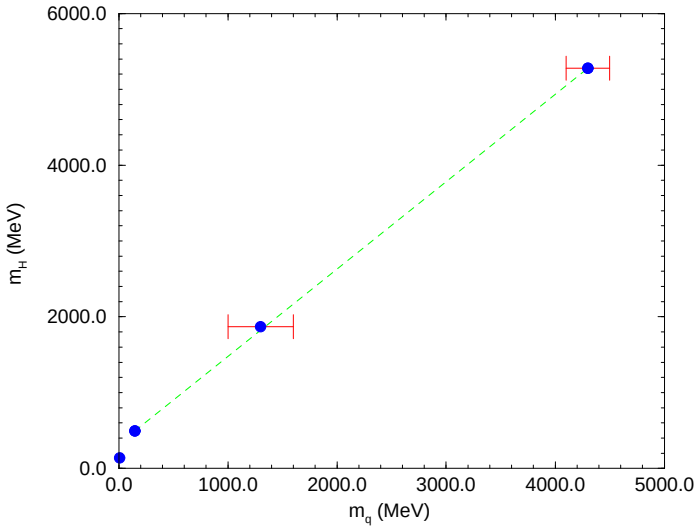

Figure 3: Pseudoscalar meson mass as a function of the mass of the heaviest constituent, $\hat{m}_q$.[9] Only the π does not lie on the same straight line.

finite temperature lattice-QCD, with the first simulations in the early eighties and extensive efforts since then.[16] The commonly used quenched approximation is inadequate for studying the phase diagram of finite temperature QCD because the details of the transition depend sensitively on the number of active (light) flavours. It is therefore necessary to include the fermion determinant.

That is even more important in the presence of μ, which modifies the fermion piece of the Euclidean action: $\gamma \cdot \partial + m \to \gamma \cdot \partial - \gamma_4 \mu + m$, and thus the fermion determinant acquires an explicit imaginary part. The $\mu \neq 0$ QCD action being complex entails that the study of finite density is significantly more difficult than that of finite temperature. Simulations that ignore the fermion determinant at $\mu \neq 0$ encounter a forbidden region, which begins at $\mu = m_\pi/2$,[10] and since $m_\pi \to 0$ in the chiral limit this is a serious limitation, preventing a reliable study of chiral symmetry restoration. The phase of the fermion determinant is essential in eliminating this artefact.[11]

The contemporary application of DSEs at finite temperature and chemical potential is a straightforward extension of the $T = 0 = \mu$ studies. The direct approach is to develop a finite-T extension of *Ansätze* for the dressed-gluon propagator. The quark DSE can then be solved and, having the dressed-quark and -gluon propagators, the response of bound states to increases in T and μ can be studied. As a nonperturbative approach that allows the simultaneous

study of DCSB and confinement, the DSEs have a significant overlap with lattice simulations: each quantity that can be estimated using lattice simulations can also be calculated using the DSEs. This means they can be used to check the lattice simulations, and importantly, that lattice simulations can be used to constrain their model-dependent aspects. Once agreement is obtained on the common domain, the DSEs can be used to explore phenomena presently inaccessible to lattice simulations.

3.1 Finite-(T,μ) Quark DSE

The renormalised dressed-quark propagator at finite-(T,μ) has the form

$$S(\vec{p},\tilde{\omega}_k) = \frac{1}{i\vec{\gamma}\cdot\vec{p}\,A(\vec{p},\tilde{\omega}_k) + i\gamma_4\,\tilde{\omega}_k C(\vec{p},\tilde{\omega}_k) + B(\vec{p},\tilde{\omega}_k)} \tag{21}$$

$$\equiv -i\vec{\gamma}\cdot\vec{p}\,\sigma_A(\vec{p},\tilde{\omega}_k) - i\gamma_4\,\tilde{\omega}_k\sigma_C(\vec{p},\tilde{\omega}_k) + \sigma_B(\vec{p},\tilde{\omega}_k) \tag{22}$$

where $\tilde{\omega}_k := \omega_k + i\mu$ with $\omega_k = (2k+1)\,\pi\,T$, the fermion Matsubara frequencies, $k \in \mathbb{Z}$. The complex scalar functions: $A(\vec{p},\tilde{\omega}_k)$, $B(\vec{p},\tilde{\omega}_k)$ and $C(\vec{p},\tilde{\omega}_k)$ satisfy: $\mathcal{F}(\vec{p},\tilde{\omega}_k)^* = \mathcal{F}(\vec{p},\tilde{\omega}_{-k-1})$, $\mathcal{F} = A, B, C$, and although not explicitly indicated they are functions only of $|\vec{p}|^2$ and $\tilde{\omega}_k^2$.

$S(\vec{p},\tilde{\omega}_k)$ satisfies the DSE

$$S^{-1}(\vec{p},\tilde{\omega}_k) = Z_2^A\, i\vec{\gamma}\cdot\vec{p} + Z_2\,(i\gamma_4\,\tilde{\omega}_k + m_{\rm bm})\; + \Sigma'(\vec{p},\tilde{\omega}_k)\,; \tag{23}$$

where the regularised self energy is

$$\Sigma'(\vec{p},\tilde{\omega}_k) = i\vec{\gamma}\cdot\vec{p}\,\Sigma'_A(\vec{p},\tilde{\omega}_k) + i\gamma_4\,\tilde{\omega}_k\,\Sigma'_C(\vec{p},\tilde{\omega}_k) + \Sigma'_B(\vec{p},\tilde{\omega}_k)\;, \tag{24}$$

$$\Sigma'_{\mathcal{F}}(\vec{p},\tilde{\omega}_k) = \int_{l,q}^{\bar{\Lambda}} \frac{4}{3}\,g^2\,D_{\mu\nu}(\vec{p}-\vec{q},\tilde{\omega}_k-\tilde{\omega}_l)\frac{1}{4}{\rm tr}\left[\mathcal{P}_{\mathcal{F}}\gamma_\mu S(\vec{q},\tilde{\omega}_l)\Gamma_\nu(\vec{q},\tilde{\omega}_l;\vec{p},\tilde{\omega}_k)\right]\;, \tag{25}$$

$\int_{l,q}^{\bar{\Lambda}} := T\sum_{l=-\infty}^{\infty}\int^{\bar{\Lambda}}\frac{d^3q}{(2\pi)^3}$ and $\mathcal{P}_A := -(Z_1^A/p^2)i\gamma\cdot p$, $\mathcal{P}_B := Z_1$, $\mathcal{P}_C := -(Z_1/\tilde{\omega}_k)i\gamma_4$.

The finite-(T,μ), Landau-gauge dressed-gluon propagator has the form

$$g^2 D_{\mu\nu}(\vec{p},\Omega) \;=\; P^L_{\mu\nu}(\vec{p},\Omega)\,\Delta_F(\vec{p},\Omega) + P^T_{\mu\nu}(\vec{p})\,\Delta_G(p,\Omega)\,, \tag{26}$$

$$P^T_{\mu\nu}(\vec{p}) := \begin{cases} 0; & \mu \text{ and/or } \nu = 4, \\ \delta_{ij} - \dfrac{p_i p_j}{|\vec{p}|^2}; & \mu,\nu = i,j = 1,2,3 \end{cases}\;, \tag{27}$$

with $P^T_{\mu\nu}(p) + P^L_{\mu\nu}(p,p_4) = \delta_{\mu\nu} - p_\mu p_\nu/\sum_{\alpha=1}^4 p_\alpha p_\alpha$; $\mu,\nu = 1,\ldots,4$.

In studying confinement one cannot assume that the analytic structure of a dressed propagator is the same as that of the free particle propagator: it must be determined dynamically. The $\tilde{p}_k := (\vec{p}, \tilde{\omega}_k)$-dependence of A and C is qualitatively important since it can conspire with that of B to eliminate free-particle poles in the dressed-quark propagator.[12] In this case the propagator does not have a Lehmann representation so that, in general, the Matsubara sum cannot be evaluated analytically. More importantly, it either complicates or precludes a real-time formulation of the finite temperature theory, which makes the study of nonequilibrium thermodynamics a very challenging problem. In addition, the $\tilde{p}_k$-dependence of A and C can be a crucial factor in determining the behaviour of bulk thermodynamic quantities such as the pressure and entropy, being responsible for these quantities reaching their respective ultrarelativistic limits only for very large values of T and μ. It is therefore important in any DSE study to retain $A(\tilde{p}_k)$ and $C(\tilde{p}_k)$, and their dependence on $\tilde{p}_k$.

3.2 Phase Transitions and Order Parameters

One order parameter for the chiral symmetry restoration transition is well known - it is the quark condensate, defined via the renormalised dressed-quark propagator, Eq. (14). An equivalent order parameter is

$$\mathcal{X} := \mathsf{Re}\, B_0(\vec{p} = 0, \tilde{\omega}_0)\,, \tag{28}$$

which makes it clear that the zeroth Matsubara mode determines the character of the chiral phase transition. An order parameter for confinement, valid for both light- and heavy-quarks, was introduced in Ref. [13]. It is a single, quantitative measure of whether or not a Schwinger function has a Lehmann representation, and it has been used[14] to striking effect in QED_3.

3.3 Study at $(T \neq 0, \mu = 0)$

Deconfinement and chiral symmetry restoration have been studied[13] in a DSE-model of two-light-flavour QCD. The quark DSE was solved using a one-parameter model[15] dressed-gluon propagator, which provides a good description of π and ρ-meson observables at $T = 0 = \mu$. The transitions are coincident and second-order at a critical temperature of $T_c \approx 150\,\mathrm{MeV}$, with the same estimated critical exponents: $\beta = 0.33 \pm 0.03$. Both the pion mass, m_π, and the pion leptonic decay constant, f_π, are insensitive to T for $T \lesssim 0.7\,T_c$. However, as $T \to T_c$, the pion mass increases substantially, as thermal fluctuations overwhelm quark-antiquark attraction in the pseudoscalar channel, until, at $T = T_c$, $f_\pi \to 0$ and there is no bound state. These results confirm those of contemporary numerical simulations of finite-T lattice-QCD [16].

3.4 Complementary study at $(T = 0, \mu \neq 0)$

The behaviour of this model at $\mu \neq 0$ has also been explored.[17] The model employs a dressed-gluon propagator with the simple form

$$\frac{\mathcal{G}(k^2)}{k^2} = \frac{16}{9}\pi^2 \left[4\pi^2 m_t^2 \delta^4(k) + \frac{1 - \mathrm{e}^{-[k^2/(4m_t^2)]}}{k^2} \right] , \tag{29}$$

where[15] $m_t = 0.69$ GeV is a mass-scale that marks the boundary between the perturbative and nonperturbative domains, and the quark DSE was solved in rainbow approximation. The solution has the form

$$S(p_{[\mu]}) := -i\vec{\gamma}\cdot\vec{p}\,\sigma_A(p_{[\mu]}) - i\gamma_4\,\omega_{[\mu]}\,\sigma_C(p_{[\mu]}) + \sigma_B(p_{[\mu]})\,, \tag{30}$$

where $p_{[\mu]} := (\vec{p}, \omega_{[\mu]})$, with $\omega_{[\mu]} := p_4 + i\mu$. There are two distinct types of solution: a Nambu-Goldstone mode characterised by $\sigma_{B_0} \not\equiv 0$; and a Wigner-Weyl mode characterised by $\sigma_{B_0} \equiv 0$.

The possibility of a phase transition between the two modes is explored by calculating the relative stability of the different phases, which is measured by the difference between the tree-level auxiliary-field effective-action:

$$\frac{1}{2N_f N_c}\,\mathcal{B}(\mu) := \tag{31}$$
$$\int_p^\Lambda \left\{ \ln\left[\frac{|\vec{p}|^2 A_0^2 + \omega_{[\mu]}^2 C_0^2 + B_0^2}{|\vec{p}|^2 \hat{A}_0^2 + \omega_{[\mu]}^2 \hat{C}_0^2} \right] + |\vec{p}|^2 \left(\sigma_{A_0} - \hat{\sigma}_{A_0}\right) + \omega_{[\mu]}^2 \left(\sigma_{C_0} - \hat{\sigma}_{C_0}\right) \right\} ,$$

where $\hat{A}$ and $\hat{C}$ represent the solution of Eq. (23) obtained when $B_0 \equiv 0$; i.e., when DCSB is absent. This solution exists for all μ. $\mathcal{B}(\mu)$ defines a μ-dependent "bag constant".[18] It is positive when the Nambu-Goldstone phase is dynamically favoured; i.e., has the highest pressure, and becomes negative when the Wigner pressure becomes larger. Hence the critical chemical potential is the zero of $\mathcal{B}(\mu)$, which is $\mu_c = 375\,$MeV. The abrupt switch from the Nambu-Goldstone to the Wigner-Weyl mode signals a first order transition.

The chiral order parameter *increases* with increasing chemical potential up to μ_c, with $\chi(\mu_c)/\chi(0) \approx 1.2$, whereas the deconfinement order parameter, $\kappa(\mu)$, is insensitive to increasing μ. At μ_c they both drop immediately and discontinuously to zero, as expected of coincident, first-order phase transitions. The increase of $\mathcal{X}$ with μ is a necessary consequence of the momentum dependence of the scalar piece of the quark self energy, $B(p_{[\mu]})$.[19] The vacuum quark condensate behaves in qualitatively the same manner as χ.

Even though the chiral order parameter *increases* with μ, m_π *decreases* slowly as μ increases, with $m_\pi(\mu \approx 0.7\,\mu_c)/m_\pi(0) \approx 0.94$. At this point

m_π begins to increase although, for $\mu < \mu_c$, $m_\pi(\mu)$ does not exceed $m_\pi(0)$, which precludes pion condensation. The behaviour of m_π results from mutually compensating increases in f_π^2 and $\langle m_R^\zeta(\bar{q}q)_\zeta\rangle_\pi$. f_π is insensitive to the chemical potential until $\mu \approx 0.7\,\mu_c$, when it increases sharply so that $f_\pi(\mu_c^-)/f_\pi(\mu = 0) \approx 1.25$. The relative insensitivity of m_π and f_π to changes in μ, until very near μ_c, mirrors the behaviour of these observables at finite-T.[13] For example, it leads only to a 14% increase in the $\pi \to \mu\nu$ decay width at $\mu \approx 0.9\,\mu_c$. The universal scaling conjecture of Ref. [20] is inconsistent with the anticorrelation observed between the μ-dependence of f_π and m_π.

Comparing the μ-dependence of f_π and m_π with their T-dependence, one observes an anticorrelation; e.g., at $\mu = 0$, f_π falls continuously to zero as T is increased towards $T_c \approx 150\,\mathrm{MeV}$. This is a necessary consequence of the momentum-dependence of the quark self energy.

Note A: In calculating these observables one obtains expressions for m_π^2 or f_π^2 and hence the natural dimension is mass-squared. Therefore their behaviour at finite T and μ is determined by

$$\mathsf{Re}(\omega^2_{[\mu]}) \sim [\pi^2 T^2 - \mu^2]\,, \tag{32}$$

where the T-dependence arises from the introduction of the fermion Matsubara frequency: $p_4 \to (2k+1)\pi T$. Hence when such a quantity decreases with T it will increase with μ, and vice-versa.[21]

The confined-quark vacuum consists of quark-antiquark pairs correlated in a scalar condensate.

Note B: Increasing μ increases the scalar density: $(-\langle\bar{q}q\rangle)$. This result is an expected consequence of confinement, which entails that each additional quark must be locally paired with an antiquark thereby increasing the density of condensate pairs as μ is increased.

For this reason, as long as $\mu < \mu_c$, there is no excess of particles over antiparticles in the vacuum and hence the baryon number density remains zero;[19] i.e., $\rho_B^{u+d} = 0\,,\ \mu < \mu_c$. This is just the statement that quark-antiquark pairs confined in the condensate do not contribute to the baryon number density.

The quark pressure, $P^{u+d}[\mu]$, can be calculated[19] and one finds that after deconfinement it increases rapidly, as the condensate "breaks-up", and an excess of quarks over antiquarks develops. The baryon-number density, $\rho_B^{u+d} = (1/3)\partial P^{u+d}/\partial\mu$, also increases rapidly, with

$$\rho_B^{u+d}(\mu \approx 2\mu_c) \simeq 3\,\rho_0\,, \tag{33}$$

where $\rho_0 = 0.16\,\mathrm{fm}^{-3}$ is the equilibrium density of nuclear matter. For comparison, the central core density expected in a $1.4\,M_\odot$ neutron star is 3.6-4.1 ρ_0.[22]

Finally, at $\mu \sim 5\mu_c$, the quark pressure saturates the ultrarelativistic limit: $P^{u+d} = \mu^4/(2\pi^2)$, and there is a simple relation between baryon-density and chemical-potential:

$$\rho_B^{u_F+d_F}(\mu) = \frac{1}{3}\,\frac{2\mu^3}{\pi^2}\,,\ \forall \mu \gtrsim 5\mu_c\,, \tag{34}$$

so that $\rho_B^{u_F+d_F}(5\mu_c) \sim 350\,\rho_0$. Thus the quark pressure in the deconfined domain overwhelms any finite, additive contribution of hadrons to the equation of state. That was anticipated in Ref. [17] where the hadron contribution was neglected. This discussion suggests that a quark-gluon plasma may be present in the core of dense neutron stars.

3.5 Simultaneous study of $(T \neq 0, \mu \neq 0)$

This is a difficult problem and the most complete study[19] to date employs a simple *Ansatz* for the dressed-gluon propagator that exhibits the infrared enhancement suggested by Ref. [5]:

$$g^2 D_{\mu\nu}(\vec{p},\Omega_k) = \left(\delta_{\mu\nu} - \frac{p_\mu p_\nu}{|\vec{p}|^2+\Omega_k^2}\right) 2\pi^3\,\frac{\eta^2}{T}\,\delta_{k0}\,\delta^3(\vec{p})\,, \tag{35}$$

with $\Omega_k = 2k\pi T$, the boson Matsubara frequency. As an infrared-dominant model that does not represent well the behaviour of $D_{\mu\nu}(\vec{p},\Omega_k)$ away from $|\vec{p}|^2 + \Omega_k^2 \approx 0$, some model-dependent artefacts arise. However, there is significant merit in its simplicity and, since the artefacts are easily identified, the model remains useful as a means of elucidating many of the qualitative features of more sophisticated *Ansätze*.

With this model, using the rainbow approximation, the quark DSE is[1]

$$S^{-1}(\vec{p},\omega_k) = S_0^{-1}(\vec{p},\tilde{\omega}_k) + \tfrac{1}{4}\eta^2\gamma_\nu S(\vec{p},\tilde{\omega}_k)\gamma_\nu\,. \tag{36}$$

A simplicity inherent in Eq. (35) is now apparent: it allows the reduction of an integral equation to an algebraic equation, in whose solution many of the qualitative features of more sophisticated models are manifest.

In the chiral limit Eq. (36) reduces to a quadratic equation for $B(\tilde{p}_k)$, which has two qualitatively distinct solutions. The Nambu-Goldstone solution, with

$$B(\tilde{p}_k) = \begin{cases} \sqrt{\eta^2 - 4\tilde{p}_k^2}\,, & \mathsf{Re}(\tilde{p}_k^2) < \frac{\eta^2}{4} \\ 0\,, & \text{otherwise} \end{cases} \tag{37}$$

$$C(\tilde{p}_k) = \begin{cases} 2\,, & \mathsf{Re}(\tilde{p}_k^2) < \frac{\eta^2}{4} \\ \frac{1}{2}\left(1 + \sqrt{1+\frac{2\eta^2}{\tilde{p}_k^2}}\right)\,, & \text{otherwise}\,, \end{cases} \tag{38}$$

describes a phase of this model in which: 1) chiral symmetry is dynamically broken, because one has a nonzero quark mass-function, $B(\tilde{p}_k)$, in the absence of a current-quark mass; and 2) the dressed-quarks are confined, because the propagator described by these functions does not have a Lehmann representation. The alternative Wigner solution, for which

$$\hat{B}(\tilde{p}_k) \equiv 0 \ , \ \hat{C}(\tilde{p}_k) = \frac{1}{2}\left(1 + \sqrt{1 + \frac{2\eta^2}{\tilde{p}_k^2}}\right) \ , \tag{39}$$

describes a phase of the model with neither DCSB nor confinement.

The relative stability of the different phases is measured by a (T,μ)-dependent vacuum pressure difference, which in the chiral limit is

$$\mathcal{B}(T,\mu) = \tag{40}$$
$$\eta^4\, 2N_c N_f \frac{\bar{T}}{\pi^2} \sum_{l=0}^{l_{\rm max}} \int_0^{\bar{\Lambda}_l} dy\, y^2 \left\{ \mathsf{Re}\left(2\bar{p}_l^2\right) - \mathsf{Re}\left(\frac{1}{C(\bar{p}_l)}\right) - \ln\left|\bar{p}_l^2 C(\bar{p}_l)^2\right| \right\},$$

with: $\bar{T} = T/\eta$, $\bar{\mu} = \mu/\eta$; l_{max} is the largest value of l for which $\bar{\omega}^2_{l_{\rm max}} \leq (1/4) + \bar{\mu}^2$ and this also specifies $\omega_{l_{max}}$, $\bar{\Lambda}^2 = \bar{\omega}^2_{l_{\rm max}} - \bar{\omega}_l^2$, $\bar{p}_l = (\vec{y}, \bar{\omega}_l + i\bar{\mu})$. The condition $\mathcal{B}(T,\mu) \equiv 0$ defines the phase boundary in the (μ,T)-plane.

Again, the deconfinement and chiral symmetry restoration transitions are coincident. For $\mu = 0$ the transition is second order and the critical temperature is $T_c^0 = 0.159\,\eta$, which using the value of $\eta = 1.06\,$GeV obtained by fitting the π and ρ masses corresponds to $T_c^0 = 0.170\,$GeV. This is only 12% larger than the value reported in Sec. 3.3, and the order of the transition is the same. For any $\mu \neq 0$ the transition is first-order. For $T = 0$ the critical chemical potential is $\mu_c^0 = 0.3\,$GeV, which is $\approx 30\%$ smaller than the result in Sec. 3.4. The discontinuity in the order parameters vanishes as $\mu \to 0$.

The quark pressure, P_q, is calculated easily in this model. Confinement means that $P_q \equiv 0$ in the confined domain. In the deconfined domain it approaches

$$P_{\rm UR} := \eta^4\, N_c N_f \frac{1}{12\pi^2}\left(\bar{\mu}^4 + 2\pi^2\bar{\mu}^2\bar{T}^2 + \frac{7}{15}\pi^4\bar{T}^4\right) , \tag{41}$$

the ultrarelativistic, free particle limit, at large values of $\bar{T}$ and $\bar{\mu}$. The approach to this limit is slow, however. For example, at $\bar{T} \sim 0.3 \sim 2\bar{T}_c^0$, or $\bar{\mu} \sim 1.0 \sim 3\bar{\mu}_c^0$, P_q is only $0.5\,P_{\rm UR}$. A qualitatively similar result is observed in numerical simulations of finite-T lattice-QCD.[16] This feature results from the persistence of the momentum dependent modifications of the quark propagator into the deconfined domain, and predicts that there is a "mirroring" of finite-T behaviour in the dependence of the bulk thermodynamic quantities on μ.

3.6 π and ρ properties

The model discussed in the last section has been used[21] to study the (T,μ)-dependence of π and ρ properties, and to elucidate other features of models that employ a more sophisticated *Ansatz* for the dressed-gluon propagator. For example, the vacuum quark condensate takes the simple form

$$-\langle\bar{q}q\rangle = \eta^3\,\frac{8N_c}{\pi^2}\bar{T}\sum_{l=0}^{l_{\rm max}}\int_0^{\bar{\Lambda}_l} dy\,y^2\,{\sf Re}\left(\sqrt{\frac{1}{4}-y^2-\tilde{\omega}_l^2}\right)\,: \tag{42}$$

at $T=0=\mu$, $(-\langle\bar{q}q\rangle)=\eta^3/(80\,\pi^2)=(0.11\,\eta)^3$. $(-\langle\bar{q}q\rangle)$ decreases with T but *increases* with μ, up to a critical value of $\mu_c(T)$ when it drops discontinuously to zero, in agreement with the behaviour reported in Secs. 3.3 and 3.4, see Note B. This vacuum rearrangement is manifest in the behaviour of the necessarily-momentum-dependent scalar part of the quark self energy, $B(\tilde{p}_k)$.

The leptonic decay constant also has a simple form in the chiral limit:

$$f_\pi^2 = \eta^2\frac{16N_c}{\pi^2}\bar{T}\sum_{l=0}^{l_{\rm max}}\frac{\bar{\Lambda}_l^3}{3}\left(1+4\,\bar{\mu}^2-4\,\bar{\omega}_l^2-\frac{8}{5}\,\bar{\Lambda}_l^2\right)\,. \tag{43}$$

Characteristic in Eqs. (42) and (43) is the combination $\mu^2-\omega_l^2$, see Note A. Without calculation, Eq. (43) indicates that f_π will *decrease* with T and *increase* with μ. This provides a simple elucidation of the results described in Secs. 3.3 and 3.4

The (T,μ)-response of the π and ρ masses is determined by the BSE

$$\Gamma_M(\tilde{p}_k;\check{P}_\ell) = -\frac{\eta^2}{4}\,{\sf Re}\left\{\gamma_\mu\,S(\tilde{p}_i+\tfrac{1}{2}\check{P}_\ell)\,\Gamma_M(\tilde{p}_i;\check{P}_\ell)\,S(\tilde{p}_i-\tfrac{1}{2}\check{P}_\ell)\,\gamma_\mu\right\}\,, \tag{44}$$

where $\check{P}_\ell := (\vec{P},\Omega_\ell)$, with the bound state mass obtained by considering $\check{P}_{\ell=0}$.

The π equation admits the solution

$$\Gamma_\pi(P_0) = \gamma_5\left(i\theta_1+\vec{\gamma}\cdot\vec{P}\,\theta_2\right) \tag{45}$$

and the calculated (T,μ)-dependence of the mass is depicted in Fig. 4.

For the ρ-meson there are two components: one longitudinal and one transverse to $\vec{P}$. The solution of the BSE has the form

$$\Gamma_\rho = \left\{\begin{array}{l}\gamma_4\,\theta_{\rho+}\\ \left(\vec{\gamma}-\frac{1}{|\vec{P}|^2}\,\vec{P}\vec{\gamma}\cdot\vec{P}\right)\,\theta_{\rho-}\end{array}\right.\,, \tag{46}$$

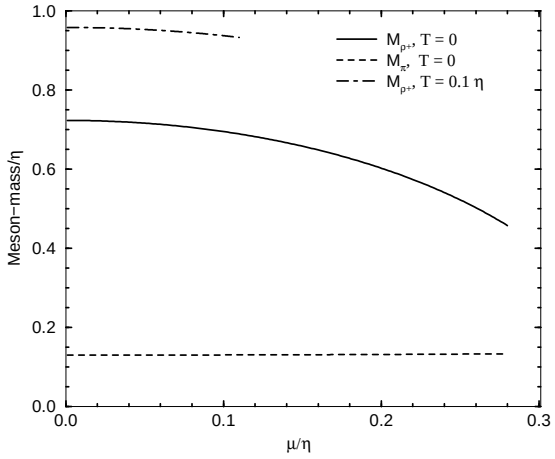

Figure 4: $M_{\rho+}$ and m_π as a function of $\bar{\mu}$ for $\bar{T} = 0, 0.1$. On the scale of this figure, m_π is insensitive to this variation of T. The current-quark mass is $m = 0.011\,\eta$, which for $\eta = 1.06\,\mathrm{GeV}$ yields $M_{\rho+} = 770\,\mathrm{MeV}$ and $m_\pi = 140\,\mathrm{MeV}$ at $T = 0 = \mu$.

where $\theta_{\rho+}$ labels the longitudinal and $\theta_{\rho-}$ the transverse solution. The eigenvalue equation obtained from (44) for the bound state mass, $M_{\rho\pm}$, is

$$\frac{\eta^2}{2}\,\mathsf{Re}\left\{\sigma_S(\omega_{0+}^2 - \tfrac{1}{4}M_{\rho\pm}^2)^2 - \left[\pm\,\omega_{0+}^2 - \tfrac{1}{4}M_{\rho\pm}^2\right]\sigma_V(\omega_{0+}^2 - \tfrac{1}{4}M_{\rho\pm}^2)^2\right\} = 1\,. \tag{47}$$

The equation for the transverse component is obtained with $[-\omega_{0+}^2 - (1/4)M_{\rho-}^2]$ in (47). Using the chiral-limit solutions, Eq. (37), one obtains immediately that

$$M_{\rho-}^2 = \frac{1}{2}\,\eta^2,\ \textit{independent}\ \text{of}\ T\ \text{and}\ \mu. \tag{48}$$

Even for nonzero current-quark mass, $M_{\rho-}$ changes by less than 1% as T and μ are increased from zero toward their critical values. Its insensitivity is consistent with the absence of a constant mass-shift in the transverse polarisation tensor for a gauge-boson.

For the longitudinal component one obtains in the chiral limit:

$$M_{\rho+}^2 = \frac{1}{2}\eta^2 - 4(\mu^2 - \pi^2 T^2)\,. \tag{49}$$

The characteristic combination $[\mu^2 - \pi^2 T^2]$ again indicates the anticorrelation between the response of $M_{\rho+}$ to T and its response to μ, and, like a gauge-

boson Debye mass, that $M^2_{\rho+}$ rises linearly with T^2 for $\mu = 0$. The $m \neq 0$ solution of Eq. (47) for the longitudinal component is plotted in Fig. 4: $M_{\rho+}$ *increases* with increasing T and *decreases* as μ increases.

Equation (47) can also be applied to the ϕ-meson. The transverse component is insensitive to T and μ, and the behaviour of the longitudinal mass, $M_{\phi+}$, is qualitatively the same as that of the ρ-meson: it increases with T and decreases with μ. Using $\eta = 1.06\,\mathrm{GeV}$, the model yields $M_{\phi\pm} = 1.02\,\mathrm{GeV}$ for $m_s = 180\,\mathrm{MeV}$ at $T = 0 = \mu$.

In a 2-flavour, free-quark gas at $T = 0$ the baryon number density is $\rho_B = 2\mu^3/(3\pi^2)$, by which gauge nuclear matter density, $\rho_0 = 0.16\,\mathrm{fm}^{-3}$, corresponds to $\mu = \mu_0 := 260\,\mathrm{MeV} = 0.245\,\eta$. At this chemical potential the algebraic model yields

$$M_{\rho+}(\mu_0) \approx 0.75 M_{\rho+}(\mu = 0)\ ,\ \ M_{\phi+}(\mu_0) \approx 0.85 M_{\phi+}(\mu = 0)\,. \tag{50}$$

The study summarised in Sec. 3.4 indicates that a better representation of the ultraviolet behaviour of the dressed-gluon propagator expands the horizontal scale in Fig. 4, with the critical chemical potential increased by 25%. This suggests that a more realistic estimate is obtained by evaluating the mass at $\mu_0' = 0.20\,\eta$, which yields

$$M_{\rho+}(\mu_0') \approx 0.85 M_{\rho+}(\mu = 0)\ ,\ \ M_{\phi+}(\mu_0') \approx 0.90 M_{\phi+}(\mu = 0)\,; \tag{51}$$

a small, quantitative modification. The difference between Eqs. (50) and (51) is a measure of the theoretical uncertainty in the estimates in each case. At the critical chemical potential for $T = 0$, $M_{\rho+} \approx 0.65\, M_{\rho+}(\mu = 0)$ and $M_{\phi+} \approx 0.80\, M_{\phi+}(\mu = 0)$.

This simple model preserves the momentum-dependence of gluon and quark dressing, which is an important qualitative feature of more sophisticated studies. Its simplicity means that many of the consequences of that dressing can be demonstrated algebraically. For example, it elucidates the origin of an anticorrelation, found for a range of quantities, between their response to increasing T and that to increasing μ. And the (T, μ)-dependence of $(-\langle\bar{q}q\rangle)$ and f_π, understood algebraically, is opposite to that observed for $m_{\rho+}$, hence the scaling law conjectured in Ref. [20] is inconsistent with this calculation, as it is with others of this type.

4 Concluding Remarks

This contribution illustrates the contemporary application of Dyson-Schwinger equations to the analysis of observable strong interaction phenomena, highlighting positive aspects and successes. Many recent, interesting studies have

been neglected: calculations of the cross section for diffractive, vector meson electroproduction;[23] the electric dipole moment of the ρ-meson;[24] and the electromagnetic pion form factor;[25] an exploration of η-η' mixing;[26] and others reviewed in Ref. [27]. However, a simple enquiry of

"http://xxx.lanl.gov/find/hep-ph"

with the keywords: "Dyson-Schwinger" or "Schwinger-Dyson", will provide a guide to other current research.

In all phenomenological applications, modelling is involved, in particular of the behaviour of the dressed Schwinger functions in the infrared. (The ultraviolet behaviour is fixed because of the connection with perturbation theory.) This is tied to the need to make truncations in order to define a tractable problem. Questions will always be asked regarding the fidelity of this modelling. The answers can only come slowly as, for example, more is learnt about the constraints that Ward Identities and Slavnov-Taylor identities in the theory can provide. That approach has been particularly fruitful in QED;[2] and already in the development of a systematic truncation procedure for the kernel of the quark DSE and meson BSE.[1] In the meantime, and as is common, phenomenological applications provide a key to understanding which elements of the approach need improvement: the approach itself must also be explored under extreme conditions.

Acknowledgments

We are grateful to the staff of the Special Research Centre for the Subatomic Structure of Matter at the University of Adelaide for their hospitality and support during this workshop. This work was supported by the US Department of Energy, Nuclear Physics Division, under contract no. W-31-109-ENG-38.

References

[1] A. Bender, C. D. Roberts and L. v. Smekal, *Phys. Lett.* B **380**, 7 (1996); C. D. Roberts in *Quark Confinement and the Hadron Spectrum II*, edited by N. Brambilla and G. M. Prosperi (World Scientific, Singapore, 1997).

[2] A. Bashir, A. Kizilersu and M.R. Pennington, *Phys. Rev.* D **57**, 1242 (1998); and references therein.

[3] C. D. Roberts and A. G. Williams, *Prog. Part. Nucl. Phys.* **33**, 477 (1994).

[4] F. T. Hawes, C. D. Roberts and A. G. Williams, *Phys. Rev.* D **49**, 4683 (1994); and F. T. Hawes, P. Maris and C. D. Roberts, in progress.

[5] N. Brown and M.R. Pennington, *Phys. Rev.* D **39**, 2723 (1989); M. R. Pennington, "Calculating hadronic properties in strong QCD", hep-ph/9611242; and references therein.
[6] P. Maris and C. D. Roberts, *Phys. Rev.* C **56**, 3369 (1997).
[7] M. A. Ivanov, Yu. Kalinovsky, P. Maris and C. D. Roberts, *Phys. Rev.* C **57**, 1991 (1998).
[8] P. Maris and C. D. Roberts in *Rostock 1997, Progress in heavy quark physics*, edited by M. Beyer, T. Mannel and H. Schröder; nucl-th/9710062.
[9] Particle Data Group (R. M. Barnett *et al.*), *Phys. Rev.* C **54**, 1 (1996).
[10] M.-P Lombardo, J. B. Kogut and D. K. Sinclair, *Phys. Rev.* D **54**, 2303 (1996).
[11] M. A. Halasz, A. D. Jackson and J. J. M. Verbaarschot, *Phys. Rev.* D **56**, 5140 (1997).
[12] C. J. Burden, C. D. Roberts and A. G. Williams, *Phys. Lett.* B **285**, 347 (1992).
[13] A. Bender, D. Blaschke, Yu. Kalinovsky and C.D. Roberts, *Phys. Rev. Lett.* **77**, 3724 (1996).
[14] P. Maris, *Phys. Rev.* D **52**, 6087 (1995).
[15] M. R. Frank and C. D. Roberts, *Phys. Rev.* C **53**, 390 (1996).
[16] F. Karsch, *Nucl. Phys.* A **590**, 376c (1995).
[17] A. Bender, *et al.*, "Deconfinement at finite chemical potential", *Phys. Lett.* B, in press.
[18] R. T. Cahill and C. D. Roberts, *Phys. Rev.* D **32**, 2419 (1985).
[19] D. Blaschke, C.D. Roberts and S. Schmidt, "Thermodynamic properties of a simple, confining model", *Phys. Lett.* B, in press.
[20] G. Brown, *Nucl. Phys.* A **488**, 689c (1988).
[21] P. Maris, C. D. Roberts and S. Schmidt, *Phys. Rev.* C **57**, R2821 (1998).
[22] R. B. Wiringa, V. Fiks and A. Fabrocini, *Phys. Rev.* C **38**, 1010 (1988).
[23] M. A. Pichowsky and T.-S. H. Lee, *Phys. Rev.* D **56**, 1644 (1997).
[24] M. B. Hecht and B. H. J. McKellar, *Phys. Rev.* C **57**, 2638 (1998).
[25] P. Maris and C. D. Roberts, "Pseudovector components of the pion, $\pi^0 \to \gamma\gamma$, and $F_\pi(q^2)$: nucl-th/9804062.
[26] D. Klabucar and D. Kekez, "η and η' at the limits of applicability of a coupled Schwinger-Dyson and Bethe-Salpeter approach in the ladder approximation": hep-ph/9710206.
[27] P. C. Tandy, *Prog. Part. Nucl. Phys.* **39**, 117 (1997).